M. Hossain*,
A. Abdkader,
A. Nocke,
R. Unger,
F. Krzywinski,
M. M. B. Hasan,
Chokri Cherif

Measurement Methods of Dynamic Yarn Tension in a Ring Spinning Process

DOI: 10.5604/12303666.1172098

Institute of Textile Machinery
and High Performance Material Technology (ITM),
TU Dresden,
Germany
E-mail: hossain@itb.mw.tu-dresden.de

Abstract
The most common measuring method to characterise the dynamic yarn path in the ring spinning process is to measure the yarn tension, where the yarn path is almost straight. However, it is much more complex to measure the yarn tension at the other positions, for example, between the yarn guide and traveller (balloon zone) and between the traveller and winding point of the cop (winding zone), as the yarn rotates continuously around the spindle axis. In this paper, two new methods of yarn tension measurement in the balloon zone are proposed. In the first method, the balloon shape was first recorded with a high speed camera. The balloon tension was then calculated by comparing the yarn strain (occurring in the balloon zone) measured by a digital image analysis program with the stress-strain curve of the yarn produced. In the second method, the radial forces of the rotating balloon were measured by using modified measurement techniques for measurement of yarn tension. Moreover a customised sensor was developed to measure the winding tension between the traveller and cop. The values measured were validated with a theoretical model and a good correlation between the measured and theoretical values could be revealed.

Key words: *balloon tension, ring spinning, winding tension, measurement method.*

Introduction

The ring spinning process is the most widely used spinning method for staple yarn production. According to the principle of the ring spinning process (***Figure 1***), a roving is fed to the drafting system in order to produce a yarn with the count required. The drafted roving is supplied through the yarn guide, called a lappet, to the ring-traveller system to impart twist to the yarn, which is wound up on the cop finally. The traveller itself rotates on the ring and is dragged with the spindle by means of the yarn that is attached to it. Each cycle of rotation of the traveller along the ring inserts one turn of twist to the yarn. The rotation of the traveller lags somewhat behind that of the spindle due to the relatively high friction of the traveller on the ring and the air drag of the traveller, as well as the thread balloon between the yarn guide and traveller. This difference in speed between the spindle and traveller enables the winding of yarn onto the cop. The yarn path can be segmented into four regions: region I - from the clamping point of delivery rollers to the yarn guide, region II - from the yarn guide to the traveller, region III - yarn passage through the traveller and region IV - from the traveller to the winding-point on the cop (***Figure 1***).

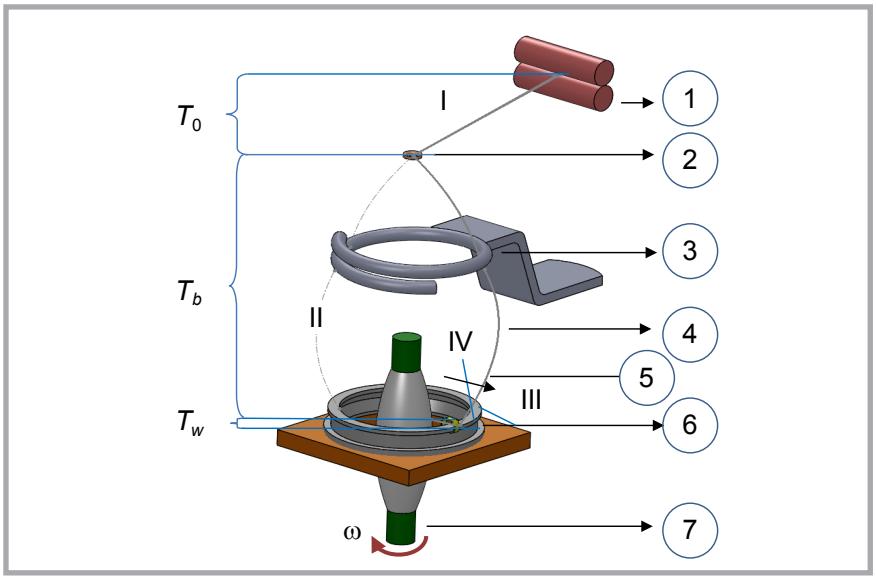

Figure 1. *Principle of ring spinning and definition of different regions in the yarn path; T_0) spinning tension, T_b) balloon tension, T_w) winding tension, I) between delivery rollers and yarn guide, II) between yarn guide and traveller, III) through traveller, IV) between traveller and winding point of cops, ω) angular velocity of spindle, 1) delivery rollers, 2) yarn guide, 3) balloon control ring, 4) yarn balloon, 5) ring, 6) traveller, 7) spibdle.*

The force generated by the motion of the traveller and the pulling of the yarn through the traveller around the spindle axis as well as the winding of the yarn onto the spinning cop causes yarn tensions, which define the actual shape of the spinning balloon. Work has to be done against the frictional force of the ring on the traveller and of the traveller on the yarn, as well as against the air drag on the traveller and on the balloon length. This work is additional to that required to overcome the friction of the spindle bearings and the air drag on the forming yarn package [1].

The tensions in the yarn during ring spinning can be considered with respect to mainly three zones (***Figure 1***) such as:

- Yarn formation zone (region I): from the nip of the delivery rollers of the drafting system to the yarn guide, the yarn tension is termed as the spinning tension (T_0) and is governed mainly due to the balloon tension at the yarn guide
- Balloon zone (region II): from the yarn guide to the traveller, tension occurs in the yarn length referred to as the balloon tension (T_b) at a given

M Hossain M, Abdkader A, Nocke A, Unger R, Krzywinski F, Hasan MMB, Cherif C. Measurement Methods of Dynamic Yarn Tension in a Ring Spinning Process.
FIBRES & TEXTILES in Eastern Europe 2016, Vol. 24, 1(115): 36-43. **DOI:** 10.5604/12303666.1172098

point on the balloon length, varying with amplitude (i.e. the radius of the point) measured from the spindle axis. The yarn in region II gives rise to dynamic forces, which determine the level of tension in the yarn and its distribution along the yarn path. The forces acting on the yarn element in this region are the yarn tension in both directions of the element, air resistance against the rotation of the balloon, the weight of the yarn, inertial forces of the relative motion, the centrifugal force, and finally the Coriolis forces.

- Winding zone (region IV): in the yarn length from the traveller to the winding point onto the cop, the yarn tension is termed as the winding tension (T_w). This yarn part is rotated according to the spindle axis on the ring-traveller-system.

The levels of yarn tension in each zone of the path are a function of spinning geometry for a definite number of spindle rotations and a definite traveller mass. The yarn tension changes continuously in all regions of its path due to the change in the parameters of spinning geometry. Therefore to track the ring spinning process and further conception for development regarding productivity, it is necessary to analyse yarn tension dynamically as a function of the main parameters of spinning geometry [2].

The dynamics as well as analysis of the yarn tension, balloon form, interactions of spinning tension and the balloon form in ring spinning have been reported by many researchers e.g. in [3 - 23]. Compared to the number of papers on the theoretical analysis of yarn dynamics, few experimental papers on yarn tension have been reported. The reason for this is partly due to the complexity of the spinning geometry [24]. The measurement of yarn tension of a running yarn moving in the length direction (e.g. in region I) is not complex and was reported in [7, 25 - 28]. The measurement of yarn winding tension in region IV was reported in [26 - 29]. In [30], the breaking force, tenacity and elongation of ballooning staple yarn were measured using a yarn ballooning rig at various rotating speeds. However, with this method the actual balloon tension occurring in the ring spinning machine cannot be compared.

In this paper, two novel methods are proposed for the measurement of yarn tension in the balloon zone during the spinning process. Moreover in order to measure the winding tension between the traveller and cop, a customised sensor was developed based on the measurement method described in [17] using non-magnetic elements, which can be further applied e.g. in the ring spinning process with a superconducting magnetic bearing (SMB) twisting system.

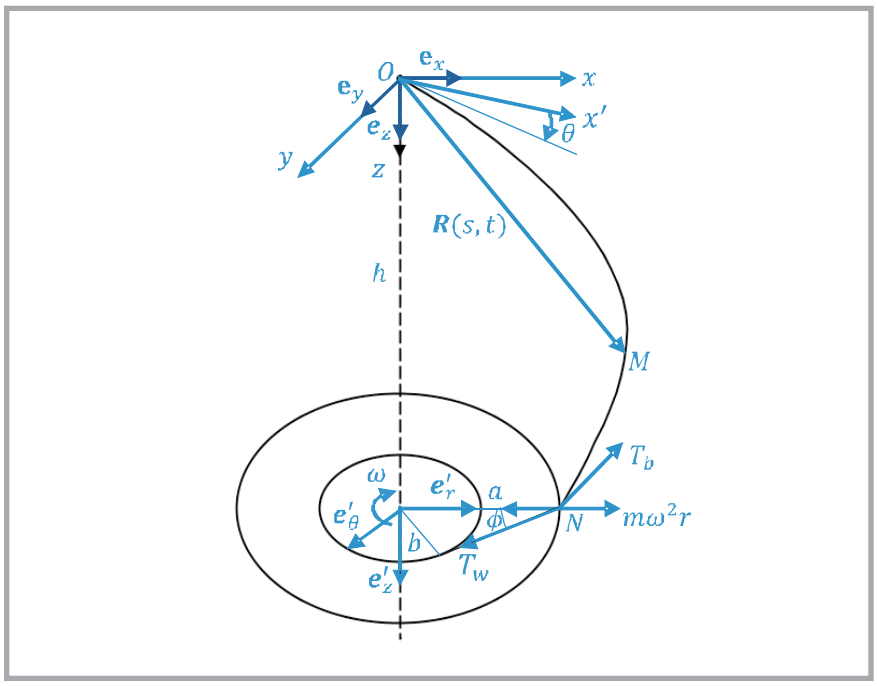

Figure 2. *Definition of coordinate systems and yarn path.*

Yarn tension prediction

The yarn path in the yarn formation zone is nearly straight, where no dynamic force occurs. The dynamical movement of yarn in the balloon zone is influenced by the centrifugal force of the yarn, The *Coriolis* force and air drag force thus determine the yarn tension distribution and related balloon shape. It is assumed that the yarn is perfectly flexible, inextensible and uniform. A rotating co-ordinate system $r(s)$, $\theta(s)$, $z(s)$ with unit vectors e_r, e_θ, e_z, was considered for the mathematical formulations of an equation for yarn path, which rotates simultaneously with the spindle axis, as shown in ***Figure 2***. $R(s, t) = re_r + ze_z$ describes the position vector of the yarn element at point M.

The well-known equation of motion for the yarn element at M can be written as ***Equation 1*** [31] where, m is the linear yarn density, ω - the spindle's angular velocity, $\mathfrak{D}^2\boldsymbol{R}$ - the yarn's acceleration, $2\omega e_z \times \mathfrak{D}\boldsymbol{R}$ - the Coriolis acceleration, $\omega^2 e_z \times (e_z \times R)$ - the yarn's centripetal acceleration, $T(s, t)$ the yarn tension at the material point; M relates to the rotating reference frame and F is the air drag force per yarn length

Equation 1 was solved with the boundary conditions (2) - (4) by the Runge-Kutta method using the boundary conditions with Matlab Software [32]. The model presented describes the yarn tension and balloon shapes in a non-normalised form considering the effect of the Coriolis force in comparison to the modelling described by Fraser el at. [31]. Finally the model was validated by measuring the yarn tension with the measuring method developed. The boundary conditions for the guide eye are:

$$r(0) = 10^{-3}m, \quad \theta(0) = 0, \quad z(0) = 0 \qquad (2)$$

The boundary condition at the traveller, N (***Figure 2***), is:

$$r(s_l) = a, \quad z(s_l) = h \qquad (3)$$

$$m\{\mathfrak{D}^2\boldsymbol{R} + 2\omega\boldsymbol{e_z} \times \mathfrak{D}\boldsymbol{R} + \omega^2\boldsymbol{e_z} \times (\boldsymbol{e_z} \times \boldsymbol{R})\} = \frac{\partial}{\partial s}\left(T\frac{\partial}{\partial s}\boldsymbol{R}\right) + \boldsymbol{F}. \qquad (1)$$

Equation 1.

Table 1. *Values of yarn tension calculated at different spindle speeds; T_0 - yarn tension between clamping point of delivery rollers and yarn guide (spinning tension-region I), T_b - yarn tension between yarn guide and traveller (balloon tension- region II), T_w - yarn tension between traveller and winding point in cop (winding tension- region IV), h - balloon height from yarn guide to ring rail, r_{max} - max. balloon diameter, h_{max} - balloon height from yarn guide at r_{max}.*

Exp., -	Spindle speed, r.p.m.	T_0, cN	T_b, cN				Balloon parameter, mm		T_w, cN
			h = 5 mm	h = 100 mm	h = 180 mm	at r_{max}	h_{max}, mm	r_{max}, mm	
1	5000	7.71	7.71	7.55	7.51	7.48	145.7	23.80	13.11
3	10000	23.22	23.69	22.59	22.39	21.96	126.3	27.40	39.48
5	15000	46.70	46.77	43.40	44.82	43.21	116.9	31.00	79.38

$$-m_T\omega^2 a e_r = -T_1 \left.\frac{dR}{ds}\right|_{s_l} - T_2 cos\phi e_r + T_2 sin\phi \overrightarrow{e_\theta} + N - \mu|N| e_\theta \quad (4)$$

$$T_b[g\sin\phi - a\theta'(s_l)] = \mu\sqrt{[T_b(r'(s_l) + g\cos\phi) - m_T\omega^2 a]^2 + [T_b z'(s_l)]^2} \quad (5)$$

Equations 4 and 5.

s_l describes the length of the yarn between the guide eye and traveller.

The other boundary condition can be derived from the equation of motion for the traveller, which can be described as ***Equation 4*** [19] where, ϕ $\left(\sin\phi = {}^{b}/_{a}\right)$ - angle between the traveller and lay point, s_l - length of yarn in the balloon, $\left.\frac{d\vec{R}}{ds}\right|_{s_l}$ - unit tangent vector to the yarn in the balloon at the traveler, N - the force the ring exerts on the traveler in the direction normal to the ring.

The boundary condition can be obtained by the elimination of N from ***Equation 4*** as ***Equation 5*** [19]: μ is the coefficient of friction between the ring and traveller, T_b the yarn tension at the bottom of the balloon, m_T the traveller mass, ϕ the wind angle (***Figure 2***), and $r'(s_l)$, $\theta'(s_l)$ and $z'(s_l)$ are the geometrical quantities of the balloon shape.

The winding tension T_w (***Figure 2***) is estimated by the EULER equation as follows

$$T_w = T_b \cdot e^{\mu_y \alpha} \quad (6)$$

where, μ_y denotes the friction between the ring and traveller, μ_y the coefficient of friction between the yarn and traveller, and α is the wrap angle (***Figure 2***).

The yarn tension in different regions of the yarn path in regions II and IV was calculated by the numerical model developed, shown in ***Table 1***. The yarn tension in region II was calculated at three different locations (such as at balloon heights of 5, 100 and 180 mm from the yarn guide to the ring rail), so that the yarn tension F(II) close to the yarn guide, balloon control ring and traveller can be predicted. For the calculation, the balloon height is considered as 180 mm. in the assumptions of the mathematical model; the effect of ring rail movement is neglected. For the modelling, we considered a constant balloon height such as 180 mm. For the validation, a measurement was also made at the same height. In any case both modelling and measurement can be done at any balloon height applicable for the existing ring spinning process. The maximal balloon diameter r_{max} and its position h_{max} are also calculated with this model, which is important for the machine construction. The maximum yarn tension occurs at region IV between the traveller and cop. This tension is higher than that of other regions due to the friction between the ring and traveller and between the yarn and traveller.

Experimental details

Parameters of yarn tension measurements

For the measurement of yarn tension, the parameters used during spinning are detailed in ***Table 2***. The experiments were done at a constant balloon height of 180 mm. An ML 55B from HBM, Germany was used as the amplifier, the signal recorded continuously with an NI Instruments LabView SignalExpress (SignalExpress (National Instruments GmbH, Germany), and evaluated by a DIAdem program (National Instruments GmbH, Germany) later on.

Measurement of yarn tension between the yarn guide and traveller (balloon zone)

Approach-I (from balloon shape)

The balloon tension is measured through the deformation behaviour of the yarn at a

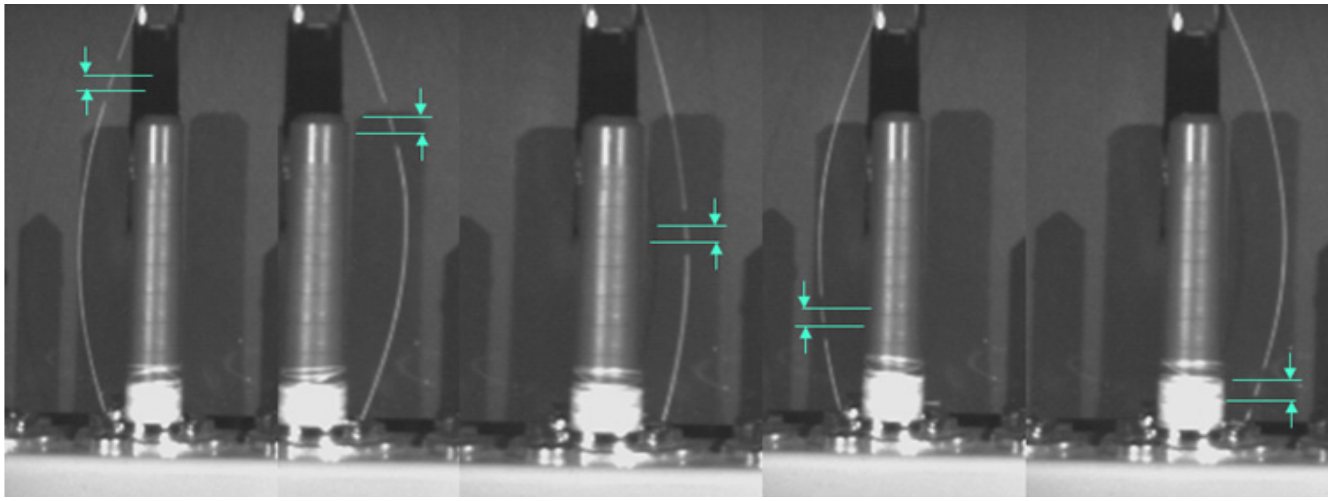

Figure 3. *Measurement of yarn strain from the balloon shape at a spindle speed of 10,000 r.p.m.*

spindle rotation of 10,000 r.p.m. based on an optical approach. Therefore yarn between the delivery rollers and yarn guide is marked in two positions with a distance of 5 mm. This length is considered as the original length l_0. The deformation behaviour of this length in the balloon zone during spinning is recorded with a high speed camera (Photron Fastcam Ultima SA-3 Photron, USA) at 15,000 fps continuously and measured at different positions between the yarn guide and traveller (***Figure 3***). The balloon shapes are taken while the traveller is situated at the position of 90° or, 270° with respect to the front view at 0°.

From the analysis of the digital image using the software Image J [21], the strain of the yarn (ε) during spinning in the balloon zone is measured using ***Equation 6***:

$$\varepsilon = \frac{l_1 - l_0}{l_0} \qquad (6)$$

where, l_1 is the length in the balloon shape measured.

On the other hand, the spun yarn was tested on a Tensile testing machine Z2.5 from Zwick GmbH & Co.KG, Germany to get the stress-strain behaviour of the spun yarn. Yarn tension i measured n the balloon zone is now determined comparing the yarn extension measured in balloon zone with the help of a strain-stress diagram, which provides the approximate values of balloon tension.

Approach-II

In this method the yarn tension in the balloon zone is measured using a modified sensor - *Tensometric-STAK 1321* (Tensometric GmbH, Germany), which consists of a sensor to measure the radial force acting on it as well as two yarn guiding elements to keep the deflection of the yarn constant (***Figure 4.a***).

From the differential angle $d\varphi$ and longitudinal forceof the yarn acting as a normal force F_N on the middle measuring position of the sensor, F_N is measured according to ***Equation 7***. The resultant radial force is measured with the help of wrap angle ($d\varphi$) (***Figure 4.b***).

$$\sin\left(\frac{d\varphi}{2}\right) \approx \frac{d\varphi}{2} = \frac{dF_N}{2F} \qquad (7)$$

In order to measure the yarn tension, first of all the sensor is calibrated statically (***Figure 4.c***). This is done by hanging a yarn of 30 tex with 10 and 20 g weights which press on the middle measuring position of the sensor. The sensor measures the radial force of the corresponding weight. The force in the longitudinal direction can be thus measured through this radial force in a way that the respective signal in the data acquisition software - Labview SignalExpress is scaled as 10 and 20 g, respectively. The sensor is positioned at the point of maximum balloon diameter derived from the theoretical modelling, where the yarn during balloon formation touches all the three positions of the sensors.

Measurement of winding tension between the traveller and cop (region IV)

Yarn tension between the traveller and winding point on the bobbin is determined with a developed measuring system. For this purpose, a measuring ring was mounted concentrically between the ring and cop. The measuring ring was positioned 1 mm higher compared to the ring-traveller system. The yarn path in the winding zone slides over the measuring ring in the direction to the cop

Table 2. *Parameters used for the measurement of yarn tension.*

Parameter	Value	Unit
Material	100% PES	-
Fiber count	1.14	dtex (g/10 km)
Staple length	38	mm
Roving count	657	tex (g/km)
Yarn count (m)	30	tex (g/km)
Spindle speed (n_s)	5,000; 10,000; 15,000	r.p.m.
Delivery speed (v)	7.14, 14.30, 21.43	m/min
Total draft	21.9	-
Twist	700	t.p.m.
Balloon height (h)	180	mm
Traveller weight m_T	63	mg
Ring radius (α)	22.5	mm
Cops radius (b)	14	mm

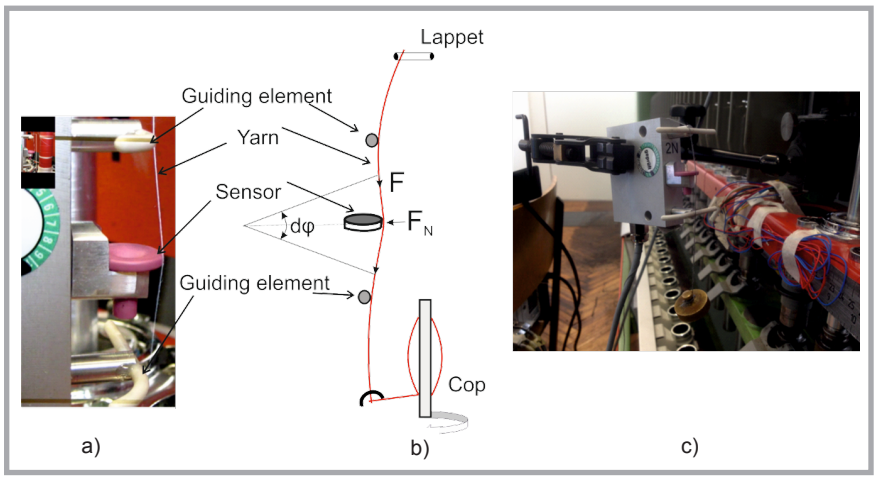

Figure 4. *a) Modified sensor Tensometric-STAK 1321 used for measurement of the balloon tension, b) schematic diagram of the principle of balloon tension measurement from the deflection angle, c) calibration of the sensor using a defined weight.*

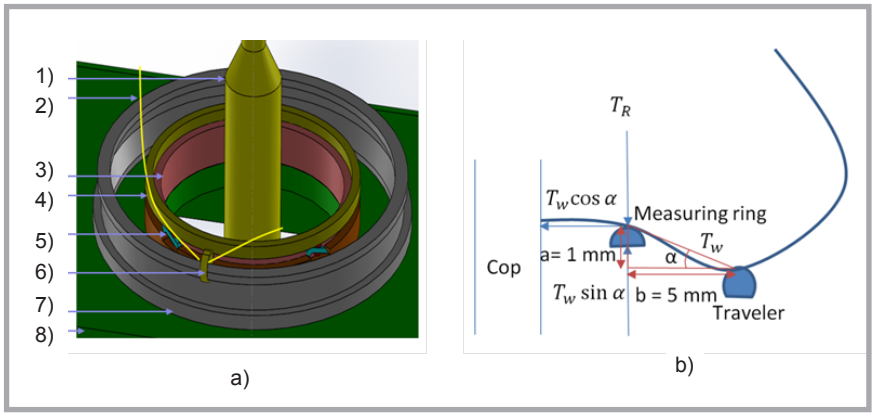

Figure 5. *a) Set-up for the measurement of yarn tension in region-IV, b) forces acting on the measuring ring and traveller by the yarn in the winding zone; 1) cops, 2) yarn, 3) supporting ring, 4) measuring ring, 5) leaf spring with strain gage, 6) traveler, 7) spinning ring, 8) ringrail.*

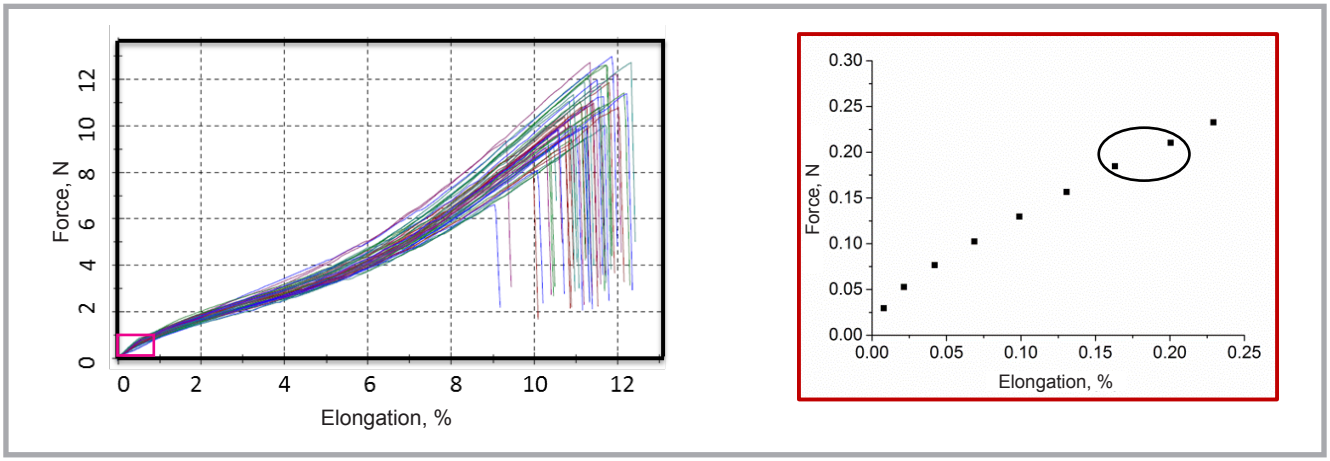

Figure 6. *a) Stress-strain curves of spun yarn measured by a Zwick tensile strength instrument and b) the balloon tension calculated from the yarn strain measured at a spindle speed of 10,000 r.p.m.*

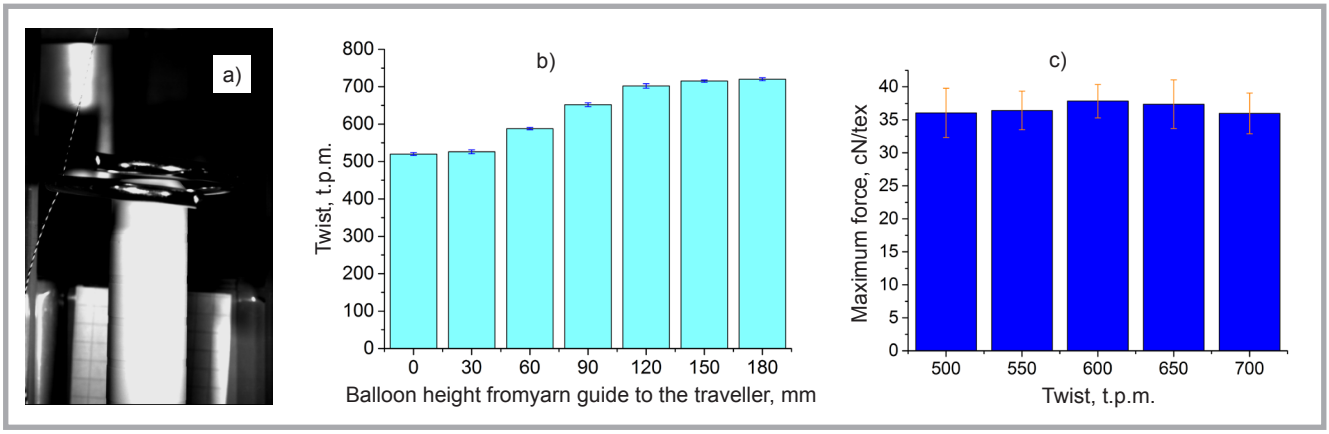

Figure 7. *a) Measurement of yarn twist in the balloon with an HS-camera, b) amount of twist at different positions of the balloon, and c) yarn strength at different amounts of twist.*

(***Figure 5.a***). The normal force (T_R) of yarn deflects the spring leaves mounted on the supporting ring. The reacting force deforms the strain-gauges fixed on the leaves, which are connected so that the same signal can be produced at each point of the measuring ring. The deflection of the strain gauges causes a change in the electrical resistance. The resonance frequency of the measuring ring is 300 Hz. During the mounting of the supporting and measuring rings, a centering device was used. The output signal is converted by a LabView data acquisition program and evaluated with a DIAdem system.

The yarn segment between the traveller and cop presses onto the measuring ring and results in a restoring force, $T_w sin\alpha$ (***Figure 5.b***). The force between the measuring ring and traveller in the tangential direction of the yarn path is T_w, where the force between the measuring ring and winding point of the cop is $T_w cos\alpha$, which is considered as the winding tension. However, the measurement was made for a constant length of the balloon, so that the angle α remains unchanged. During the calibration, the dead weights of 10 and 20 g were taken, hung over the measuring ring and scaled in LabView SignalExpress accordingly.

Results and discussion

Yarn tension (Region II)

Approach-I

A stress-strain diagram of the manufactured yarn measured by Zwick is illustrated in ***Figure 6.a***.

The strain % measured using digital analyses are compared with the same strain value obtained from the stress-strain diagram. As an example, the strain % at different positions of the balloon lies between 0.14 and 0.16 after analysing the corresponding balloon shape at a spindle speed of 10,000 r.p.m. This range of strain % was focused on in the stress-strain curve with the help of a testXpert® II program from Zwick GmbH & Co. KG (Germany), as illustrated in ***Figure 6.b***, and finally the corresponding value of force is taken as the balloon tension. As shown in ***Figure 6.b***, the balloon tension lies within the range of 22 ±2 cN at a spindle speed of 10,000 r.p.m. Similarly the balloon tension measured at a spindle speed of 5,000 and 15,000 r.p.m. is found to be 6 and 45 cN with 4% variation, respectively. The variation in balloon tension at a lower spindle speed is more, as the strain of yarn is too small to be measured. However, the yarn tension varies to a small degree within different positions of the balloon height. Moreover the amount of twist was measured at different positions of the balloon during spinning with the help of an HS-camera, as shown in ***Figure 7.a***. For this purpose, a contrast fibre was inserted before the delivery roller during the normal spinning process and recorded with the HS-camera at different positions of the balloon. Then the twist is measured

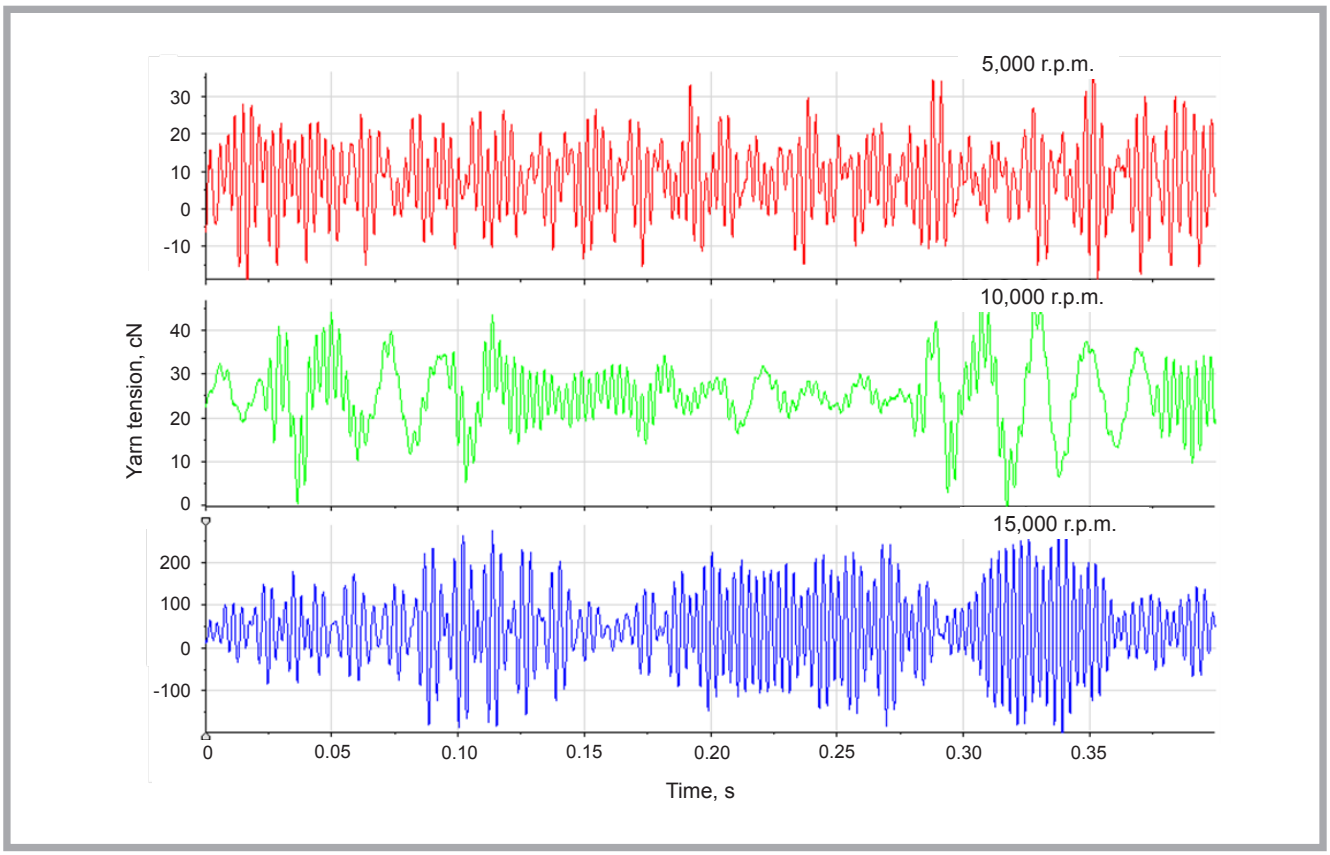

Figure 8. *Course of balloon tension over time measured by a Tensometric-STAK 1321 at different spindle speeds (approach-II).*

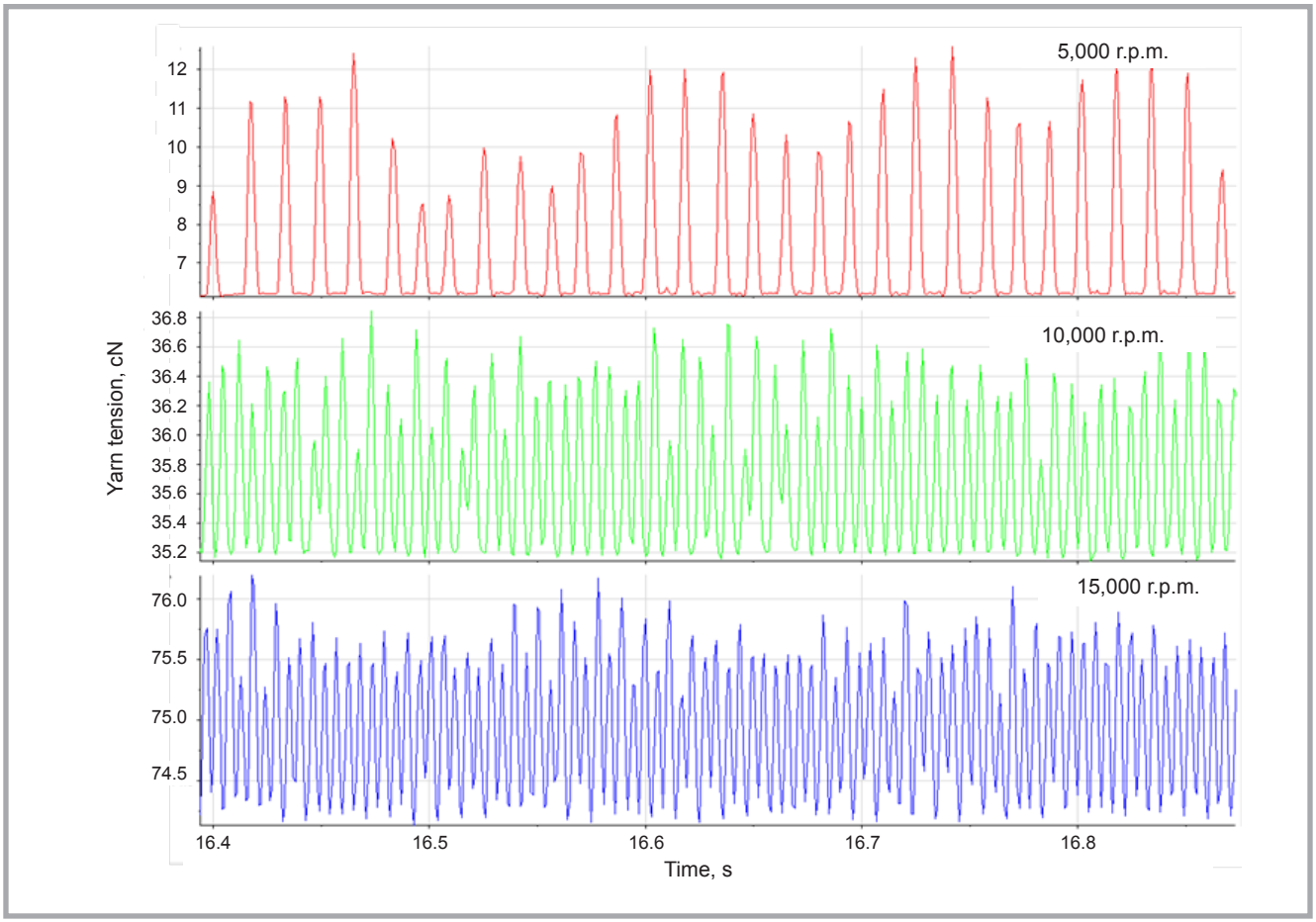

Figure 9. *Winding tension at a spindle speed of 5,000, 10,000 and 15,000 r.p.m. measured at region IV.*

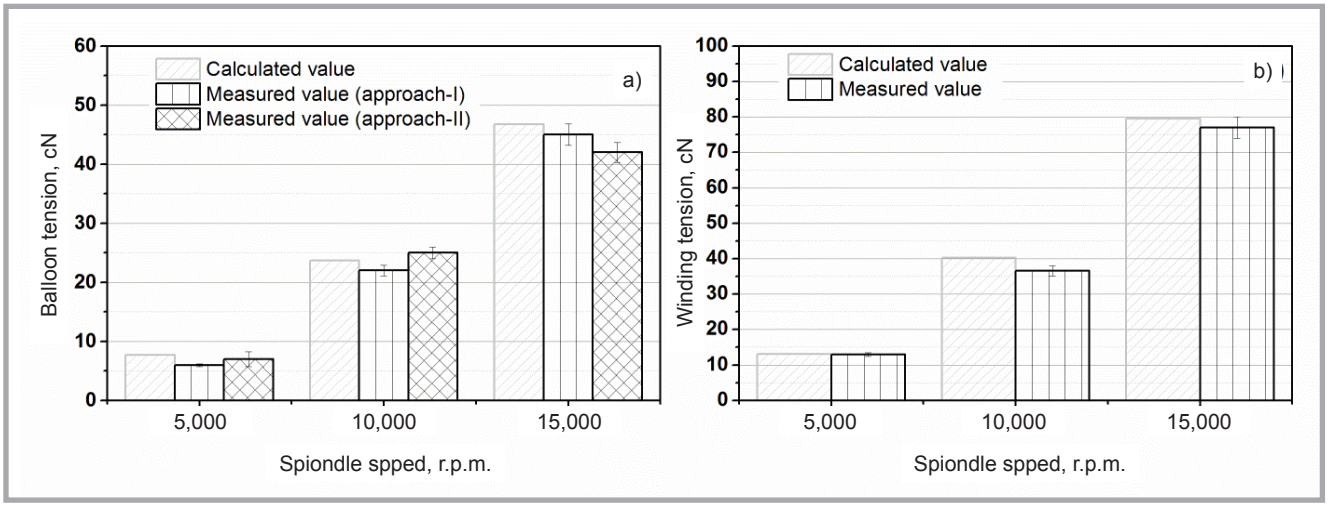

Figure 10. *Comparison of (a) balloon tension and (b) winding tension measured with values calculated at different spindle speeds.*

with the help of digital imaging software - Image J [21]. The twist measured at different positons of the balloon length is illustrated in ***Figure 7.b***. According to ***Figure 7.b***, it can be clearly seen that the twist varies along the balloon and decreases from the traveller to the yarn guide along the balloon length.

In order to find the effect of twist on the yarn strength, yarns (of 30 tex) were spun with different amounts of twist ranging from 500 to 700 t.p.m. and a tensile strength test was conducted according to DIN EN ISO 2062. The maximum breaking force in dependence on different levels of twist can be seen from ***Figure 7.c***. However, yarn strength with different amounts of twist is found to be statistically insignificant for this range of twist variation.

Therefore the method of measuring balloon tension using the force-elongation curve of the spun yarn gives a good approximation of the actual balloon tension during the spinning process.

Approach-II

The course of balloon tension measured at different spindle speeds is illustrated in ***Figure 8*** (see page 41). The tension was measured at the maximum balloon diameter. From ***Figure 8***, it can be seen that the balloon tension increases with an increase in the spindle speed, as expected. The mean yarn tension at a spindle speed of 5,000, 10,000 and 15,000 r.p.m. is found to be 7, 25 and 42 cN with 4% variation, respectively. It is observed that the shape of the balloon deforms just after touching the sensor and a vibration in the balloon is introduced, which, in turn, influence the normal rotational behaviour of the balloon and causes the variation in balloon tension.

Yarn tension (Region IV)

Results of the winding tension at spindle speeds of 5,000, 10,000 and 15,000 r.p.m. are presented in ***Figure 9*** (see page 41)**.** In this case, the signal of one of the four strain gauges is illustrated as an example. The peaks shown in ***Figure 9*** are caused by the rotation of the yarn over the measuring ring. The resultant highest peaks occur when the yarn presses right onto the spring leaves, thereby causingthe highest deformation of the spring leaves as well as strain gauges mounted on them. The winding tension was measured as 13, 36.6 & 77 cN with a variation of 5% for 5,000, 10,000 and 15,000 r.p.m, respectively. The variation in yarn tension during the measurements can be attributed to the dynamic friction between the rotating yarn and measuring ring, as well as to the tilting movement of the traveller and the eccentricity of the measuring ring.

Conclusions and outlook

In this research work different approaches to measuring yarn tension in the balloon and winding zones were developed. Measurements were performed at different spindle speeds such as 5,000, 10,000 and 15,000 r.p.m. Furthermore the values measured were validated with values calculated from a model developed for the prediction of yarn tension at different zones [32] (cf. ***Figure 10***).

From ***Figure 10***, it can be seen that the values measured have a good correlation with the values calculated. However, the values measured are generally found to be smaller than that the one calculated. The reason lies in the case of approach-I in the variation of strain measurement using digital image analysis. The force distribution along the balloon length and along the straight line within the tensile testing machine is different due to the influence of different amounts of twist. According to the model presented, yarn tension along the balloon length varied by 2%. The measurement method provides an approx. value of tension measured on the basis of the yarn extension principle. For more precision, further investigations will be made considering the level of twist at different positions of the balloon. On the other hand, the difference between calculated and measured values in the case of approach-II is the result of the dynamic friction occurring between the rotating balloon and measuring sensor, which is not considered for theoretical yarn tension prediction.

In approach-I, the measurement method can also generally be applied for higher spindle speeds. However, the movement of the ring rail causes a variation in yarn tension in the case of approach-II. Moreover the lower resonance frequency of the modified sensor used in approach-II can cause limitations to measurements at higher spindle speeds. It should be mentioned that a friction free superconducting magnetic bearing (SMB) is being implemented in a ring spinning machine at the Institute of Textile Machinery and High Performance Material Technology

(ITM) [34, 35].The results of the investigations reported in this paper will help to measure dynamic yarn tensions while using a SMB in the near future.

Acknowledgement

This research work is supported by the German Research Foundation, DFG (Project Nr. CH 174/33-1). The authors would like to thank DFG for the financial support.

References

1. Lawrence CA. *Fundamentals of spun yarn technology*. CRC Press, 2003, pp. 267, 449.
2. Skenderi Z, Orešković V, Perić P, Kalinovčić H. Determining yarn tension in ring spinning. *Text. Res. J.* 2001; 71: 343-350.
3. Barr AD, Catling H. *Manual of Cotton Spinning: The Principles and Theory of Ring Spinning*. Textile Institute, Manchester, England.
4. Batra SK, Ghosh TK, Zeidman MI. An Integrated Approach to Dynamic Analysis of the Ring Spinning Process Part I: Without Air Drag and Coriolis Acceleration. *Text. Res. J.* 1989; 59: 309-317.
5. Zhu F, Hall K, Rahn CD. Steady state response and stability of ballooning strings in air. *International journal of non-linear mechanics* 1998; 33: 33-46.
6. Bracewell GM, Greenhalgh K. Dynamical analysis of the spinning balloon. *J. Text. I. Transactions* 1953; 44: T266-T292.
7. Barr AD. A descriptive account of yarn tensions and balloon shapes in ring spinning. *J. Text. I. Transactions* 1958; 49: T58-T88.
8. Barr AD. the physics of yarn tensions and balloon shapes in spinning, winding and similar processes. *J. Text. I. Transactions* 1960; 51: T17-T38.
9. Barr AD. The Role of Air Drag in Ring Spinning. *J. Text. I. Proceedings* 1961; 52: P111-P111.
10. Sharma R, Rahn CD. An experimental study of ballooning yarn with a control ring. *J. Text. I.* 1998; 89: 621-634.
11. Tang ZX, Wang X, Fraser WB, Wang L. An experimental investigation of yarn tension in simulated ring spinning. *Fibers and polymers* 2004; *5*: 275-279.
12. Stasiak M, Michalak M. Tribilogy of Three-Element: Traveller-Ring-Yarn Friction Arrangement in Ring Spinning. Reaction of Ring to Traveller in Two-Contact Configuration. Part I. *Fibres & Textiles in Eastern Europe* 1996; 4, 2(13): 28-33.
13. Stasiak M, Michalak M. Tribology of Three-Element, Traveller-Ring-Yarn Friction Arrangements in Ring Spinning. Reaction of Ring to Traveller in Two-Contact Interaction. Part II. *Fibres & Textiles in Eastern Europe* 1996; 4, 3-4(14-15): 59-61.
14. Stasiak M, Michalak M. Tribology of Three-Element Traveller-Ring-Yarn Friction Arrangement (TRY) in Ring-Spinning Frames. Part III. Ring-Traveller Interaction under Conditions of Three-Point Contact. *Fibres & Textiles in Eastern Europe* 1997; 5, 3(18): 42-45.
15. Stasiak M, Michalak M. The Problem of Empirical Adequacy of a Model of the Friction Trio TRY (Traveller-Ring-Yarn) under Conditions of Spindle Eccentricity on a Ring Wool-Spinning Frame. *Fibres & Textiles in Eastern Europe* 1998; 6, 1(20): 28-31.
16. Stasiak M, Michalak M. The Complementary Relationship Between the Dynamic and Thermal Conditions of the Friction Trio (Traveller-Ring-Yarn) and the Degree of Wear of Its Elements. *Fibres & Textiles in Eastern Europe* 1998; 6, 2(21): 36-38.
17. Przybył K. Dynamics of Yarn in the Process of Its Formation on the Ring-spinning Machine. *Fibres & Textiles in Eastern Europe* 1995; 3, 3(10): 36-38.
18. Przybyl K. Modelling Yarn Tension in the Process of Manufacturing on the Ring-Spinning Machine. Fibres & Textiles in Eastern Europe 1998; 6, 3(22): 30-33.
19. Przybył K. Simulating the Dynamics of the Twisting-and-Winding System of the Ring Spinning Frame. *Fibres & Textiles in Eastern Europe* 2001; 9, 1(32): 16-19.
20. Przybył K. Stability of Working Conditions of the Twisting-and-Winding System of the Ring Spinning Frame in Dependence on Yarn Material. *Fibres & Textiles in Eastern Europe* 2001; 9, 4(35): 24-27.
21. Przybył K. Influence of Yarn Surface Properties on the Dynamic of the Twisting-and-Winding System of the Ring Spinning Frame. *Fibres & Textiles in Eastern Europe* 2002; 10, 2(37): 27- 31.
22. Przybył K. Stable Working Conditions of the Twisting-and-Winding System of a Ring Spinning Frame. *Fibres & Textiles in Eastern Europe* 2005, 13, 1(49) 35-38.
23. Przybył K. Influence of changes in Yarn Twist on the Dynamics of Yarn Motion During Spinning on a Ring Spinning Machine. *Fibres & Textiles in Eastern Europe* 2008, 16, 2(67) 23-26.
24. Klein W. Die Spinngeometrie und ihre Bedeutung. *Int. Textile Bull.* 1993; 39.
25. Bühler G, Schenkel E. Können ringspinnmaschinen schneller spinnen und trotzdem weniger Fadenbruche haben? *Melliand Textilber* 1974; 55: 91-100.
26. Sonntag E. Einsatz computerunterstützter Messtechnik zur Systemanalyse des Ringspinnprozesses, Teil I: Die Sensorik. *Melliand Textilber* 1993; 74: 1207-1212.
27. Sonntag E. Einsatz computerunterstützter Messtechnik zur Systemanalyse des Ringspinnprozesses, Teil II: Die Messsignalverarbeitung. *Melliand Textilber* 1994; 75: 223-350.
28. Sonntag E. Einsatz computerunterstützter Messtechnik zur Systemanalyse des Ringspinnprozesses, Teil III: Messungen an einer Hochgeschwindigkeitsringspinnmaschine. *Melliand Textilber* 1994; 75: 350-354.
29. Lünenschloß J, Bünger, CM. Neues Verfahren zur Ermittlung der Fadenzugkraft in der Aufwindezone beim Ringspinnen bzw. Ringzwirn. *Melliand Textilberichte* 1984; 5: 297-299.
30. Tang ZX, Wang L, Fraser WB, Wang X. In-situ tensile properties of a ballooning staple yarn. *Text. Res. J.* 2009; 79: 548-554.
31. Fraser WB. On the Theory of Ring spinning. *Philosophical transactions Royal Society London* 1993; 342: 439-468.
32. Hossain M, Telke Ch, Abdkader A, Cherif Ch and Beitelschmidt M. Modelling and simulation of yarn path using sensitivity analysis in the spinning process. In: *15th AUTEX World Textile Conference,* 2015, June10-12, 2015, Bucharest, Romania.
33. http://imagej.nih.gov/ij/ (accessed 06.07.2015).
34. Hossain M, Abdkader A, Cherif C, et al. Innovative twisting mechanism based on superconducting technology for higher productivity in ring spinning machine. *Text. Res. J.* 2014; 84: 871-880.
35. Hossain M, Abdkader A, Cherif C, Berger D, Fuchs G, Schultz L. High performance ring spinning using superconducting magnetic bearing system. In: *13th AUTEX World Textile Conference*, 2013.

Received 20.06.2014 Reviewed 15.09.2015